ESC European Society of Cardiology

European Heart Journal - Cardiovascular Imaging (2019) **20**, 75–83
doi:10.1093/ehjci/jey035

Optical coherence tomography-verified morphological correlates of high-intensity coronary plaques on non-contrast T1-weighted magnetic resonance imaging in patients with stable coronary artery disease

Tomoaki Kanaya[1], Teruo Noguchi[1]*, Fumiyuki Otsuka[1], Yasuhide Asaumi[1], Yu Kataoka[1], Yoshiaki Morita[2], Hiroyuki Miura[1], Kazuhiro Nakao[1], Masashi Fujino[1], Tomohiro Kawasaki[3], Kunihiro Nishimura[4], Teruo Inoue[5], Jagat Narula[6], and Satoshi Yasuda[1]

[1]Department of Cardiovascular Medicine, National Cerebral and Cardiovascular Center, 5-7-1 Fujishirodai, Suita, Osaka, 565-8565, Japan; [2]Department of Radiology, National Cerebral and Cardiovascular Center, 5-7-1 Fujishirodai, Suita, Osaka, 565-8565, Japan; [3]Cardiovascular Center, Shin-Koga Hospital, Kurume, Japan; [4]Department of Preventive Medicine, National Cerebral and Cardiovascular Center, 5-7-1 Fujishirodai, Suita, Osaka, 565-8565, Japan; [5]Department of Cardiovascular Medicine, Dokkyo Medical University Hospital, 880 kitakobayashi, Mibu, Tochigi, 321-0293, Japan; and [6]Icahn School of Medicine at Mount Sinai, 1190 Fifth Avenue New York, NY 10029, USA

Received 8 June 2017; editorial decision 12 February 2018; accepted 14 February 2018; online publish-ahead-of-print 5 March 2018

Aims Coronary high-intensity plaques (HIPs) with a high plaque-to-myocardial signal intensity ratio (PMR) on non-contrast T1-weighted imaging in patients with stable coronary artery disease (CAD) are associated with future coronary events. To characterize the morphological substrate of HIP, we performed a correlative optical coherence tomography (OCT) study.

Methods and results We examined 137 lesions in 105 patients with stable angina pectoris or silent myocardial ischaemia scheduled for percutaneous coronary intervention (PCI) using a 3 T magnetic resonance scanner. Pre-interventional OCT was performed for PCI target lesions. HIP was defined as PMR $\geq$ 1.4. Of the 137 lesions, 34% were HIP and 66% were non-HIP. The prevalence of lipid-rich plaque (96% vs. 70%, $P < 0.001$), macrophage accumulation (65% vs. 46%, $P = 0.046$), cholesterol crystals (46% vs. 22%, $P = 0.006$), and healed plaque rupture (multiple layers of different optical densities overlaying a large lipid accumulation, 72% vs. 18%, $P < 0.001$) was significantly higher in the HIP group than the non-HIP group; no significant differences were observed for the presence of thin cap fibroatheroma, intracoronary thrombus, and plaque rupture between the two groups. Multivariable stepwise logistic regression analysis showed that HIP was significantly associated with the presence of healed plaque rupture [odds ratio (OR) 9.32; 95% confidence interval (95% CI) 4.05–22.71; $P < 0.001$] and lipid-rich plaque (OR 4.38; 95% CI 1.08–29.77; $P = 0.038$).

Conclusions The significant association between HIP- and OCT-derived healed plaque rupture and large lipid core provides new insights into the characteristics of high-risk plaques, even in clinically stable CAD.

Keywords coronary artery disease • magnetic resonance imaging • optical coherence tomography • myocardial infarction

* Corresponding author. Tel: +81-6-6833-5012; Fax: +81-6-6872-7486. E-mail: tnoguchi@ncvc.go.jp

Introduction

Magnetic resonance imaging (MRI) of the coronary vessels allows for the characterization of the extent of luminal stenosis, plaque burden, and plaque instability.[1] Recently, the presence of a high-intensity plaque (HIP) with a plaque-to-myocardial signal intensity ratio (PMR) of ≥1.4 was shown to be a predictor of future coronary events in patients with stable coronary artery disease (CAD).[2] Coronary HIPs with high PMR are found in up to one-third (28–36%) of patients with stable CAD.[2,3] However, the mechanisms underlying the association between these lesions and adverse outcomes in patients with stable CAD are not fully understood.

To define the morphological substrate of atherosclerotic coronary plaques producing HIPs with high PMR, we used intracoronary optical coherence tomography (OCT) to precisely identify underlying plaque characteristics.[4–6] An *ex vivo* post-mortem histopathological study confirmed the accuracy of OCT for identifying various features of high-risk plaques including thin cap fibroatheroma (TCFA), lipid-rich core, inflammation, neovascularization, healed plaque rupture, and luminal narrowing.[4–10]

Methods

Study population and percutaneous coronary intervention procedure

Between October 2012 and November 2016, 140 consecutive patients with stable angina pectoris (SAP) or silent myocardial ischaemia with >70% computed tomography angiography (CTA)-verified significant coronary artery stenosis were scheduled for elective percutaneous coronary intervention (PCI). They were prospectively enrolled in this study and underwent non-contrast T1-weighted imaging (T1WI) on cardiac magnetic resonance (CMR) within 24 h of the scheduled PCI and OCT procedures. All patients had demonstrated inducible myocardial ischaemia on stress myocardial scintigraphy and met the appropriate criteria for coronary intervention. We excluded 35 patients because OCT could not be performed before PCI ($n = 27$), CMR or OCT image quality was poor ($n = 4$; chronic atrial fibrillation in 1 patient and heart rate > 75 b.p.m. despite oral β-blocker therapy in 3 patients), or chronic kidney disease stage ≥3 was present ($n = 4$). Thus, 105 patients, consisting of 61 with stable effort angina pectoris and 44 with silent myocardial ischaemia, were evaluated in this correlative study. PCI was performed after intravenous administration of 10 000 IU heparin using a 6 Fr sheath and catheters. The target lesion was selected based on the presence of myocardial ischaemia diagnosed with stress myocardial scintigraphy. Antiplatelet therapy before PCI consisted of aspirin (100 mg) and clopidogrel (75 mg) for at least 7 days. This study was approved by the institutional review board of the National Cerebral and Cardiovascular Center. Written informed consent was obtained from all patients.

CMR protocol

Non-contrast T1WI was performed on a 3 T MR system with a 32-channel cardiac coil (MAGNETOM Verio; Siemens AG Healthcare Sector, Erlangen, Germany). The procedures used to acquire MR images in this study have been previously described.[11,12] Briefly, coronary plaque imaging was performed using an inversion recovery-prepared 3D T1W turbo fast low-angle shot sequence with an electrocardiographic trigger, navigator-gated free-breathing, and fat suppression. Transaxial sections covered the entire heart (inversion time 650 ms; field of view 280 × 228 mm; acquisition matrix 256 × 187; reconstruction matrix 512 × 374; acquisition slice thickness 1.0 mm; reconstruction spatial resolution 0.6 × 0.5 × 0.6 mm; repetition time/echo 4.7 ms/2.13 ms; flip angle 12°; GRAPPA factor 2; navigator gating window ±1.5–2.5 mm; and data acquisition window 84–120 ms). Trigger delay and acquisition window were based on the duration of minimal right coronary artery motion as determined on cine-MR imaging. The mean acquisition time for plaque imaging was 23 ± 3 min.

CMR image analysis

PMR was defined as the signal intensity of the coronary plaque divided by the signal intensity of nearby left ventricular myocardium. The methods used to evaluate plaque images in this study have been described previously.[2,13] Two experienced investigators unaware of patient data used the T1 weighted images to calculate PMR independently. The highest signal intensity detected in each plaque was considered the PMR value for that plaque in segment-based analysis. In patient-based analysis, the highest PMR among the coronary plaques was defined as the PMR for that subject. A coronary plaque with PMR ≥ 1.4 was defined as a HIP. A coronary plaque with PMR < 1.4 was defined as a non-HIP since coronary plaques with PMR ≥ 1.4 have been shown to be associated with poor clinical prognosis in a previous study.[2]

To confirm that the location of an observed HIP corresponds to the presence of a coronary plaque, we used cross-sectional and reconstructed curved multiplanar CTA images. In addition, for plaque detection, we used co-registration images to facilitate confirmation of the anatomical position of high-intensity lesions on T1-weighted images and the coronary vessel on a standard console of a clinical MR system.[2,13] The location of a non-HIP lesion was determined by carefully comparing the CTA and MRA images or invasive coronary arteriography (CAG) images during PCI using fiduciary points (e.g. side branches). Once a non-HIP lesion had been confirmed with both CTA and coronary MR angiography, the corresponding areas on coronary T1-weighted images were carefully matched using the surrounding cardiac and chest wall structures.[14]

To exclude breathing artefacts, the signal-to-noise ratio was defined as signal intensity (myocardium)/signal intensity (background), where background indicates extracorporeal background without artefacts. Plaque lesions with signal-to-noise ratio < 3 were excluded from the analysis.

Intraclass correlation coefficients with 95% confidence intervals (95% CIs) were calculated to assess intrareader and inter-reader agreement for PMR. The interval between initial analysis of PMR of HIPs and secondary analysis was 3 months. The intrareader intraclass coefficient was 0.947 (95% CI 0.911–0.969). The inter-reader intraclass correlation coefficient was 0.916 (95% CI 0.866–0.957). All correlation coefficients for PMR were >0.8 and had narrow CIs, indicating good intraobserver and interobserver agreement.

OCT image acquisition

Intravascular OCT of the entire target vessel was performed before PCI as follows.[15] After intracoronary administration of nitroglycerin (100–300 μg), a commercially available frequency-domain OCT system (ILUMIEN/ILUMIEN OPTIS OCT Intravascular Imaging System, St. Jude Medical, St. Paul, MN, USA) was advanced to the distal site of a target lesion. OCT pullback was performed at 20 mm/s with continuous injection of contrast media through the guiding catheter. The raw OCT data were anonymized and digitally stored in offline review systems (St. Jude Medical) for subsequent analysis.

OCT data analysis

OCT image analysis was performed by two experienced observers who were blinded to the clinical data using previously established criteria for

OCT plaque characterization.[5,6,16,17] Non-target coronary plaques with 20–70% diameter stenosis in the same vessel as target lesions on quantitative CAG and target lesions undergoing PCI were analysed. Because OCT examination is an invasive technique performed during PCI, coronary vessels without target lesions for PCI were therefore excluded. The presence of lipid, TCFA, plaque rupture, calcification, thrombus, macrophage accumulation, cholesterol crystals, and microchannels on OCT images were evaluated within a 10 mm segment (5 mm proximal to 5 mm distal to the target lesion at the smallest lumen cross-sectional area), in accordance with previous studies.[5,14,18] If the two observers had discordant diagnoses, a consensus diagnosis was obtained using repeated offline readings. When lipid, characterized by signal-poor regions with diffuse borders, was present for >90° in any cross-sectional images, the plaque was considered lipid-rich. For each plaque, fibrous cap thickness was measured three times at its thinnest part and the average value was calculated. TCFA was defined as lipid-rich plaque with cap thickness ≤65 μm. Lipid core length was defined as the longitudinal length of contiguous cross-sections that fulfilled the definition of lipid-rich plaque. Plaque rupture was defined as intimal interruption and cavity formation in a plaque. Calcification was defined as a well-delineated signal-poor region with sharp borders. Thrombus was defined as an irregular mass with high or low backscattering protruding into the lumen. Thrombus type was further classified as either red or white. Red thrombus was defined as a high backscattering protrusion with signal-free shadowing on OCT. White thrombus was defined as a signal-rich, low backscattering projection. Macrophage accumulation was defined as bright spots with high OCT backscattering signal variances. A microchannel was defined as a black hole or tubular structure within a plaque observed on ≥3 consecutive cross-sectional images. Healed plaque rupture was detected as a landmark with multiple tissue layers of different optical densities overlying a large lipid core in the presence or absence of calcification.[9] A cholesterol crystal was defined as a thin linear region of high signal intensity within a lipid plaque.[17] Interobserver and intraobserver variability were assessed based on the evaluation of all images by two independent readers and by the same reader at two separate time points, respectively.

CTA scanning and analysis

Coronary CTA was performed using a dual-source CT scanner (SOMATOM Definition Flash, Siemens Healthcare, Erlangen, Germany). Coronary images were acquired with 128 × 0.6-mm slice collimation, 280-ms gantry rotation time, 120-kV tube voltage, and 280-mAs quality reference current–time product. The images were reconstructed with 0.6-mm slice thickness in 0.3-mm increments with a medium smooth convolution kernel (B26f). Quantitative lesion analysis was performed using software that facilitates plaque volume measurement (Ziostation2, Ziosoft, Tokyo, Japan). Parameters assessed included (i) plaque volume; (ii) remodelling index (RI) with plaques that have RI ≥ 1.10 considered to be within an artery with positive remodelling[19]; (iii) spotty calcification; and (iv) Hounsfield units (HU), which was coded by the software as low-attenuation plaques (LAPs) (<30 HU), intermediate attenuation plaques (30–150 HU), calcified plaques (351–1000 HU), and lumen (151–350 HU) based on colour.[20] The CT density of the plaques of at least three points was assessed and averaged.[21] Spotty calcification was defined as <3 mm on focal multiplanar reconstruction images and cross-sectional images.[13,19]

Statistical analyses

Continuous variables are presented as means ± SD for normally distributed variables, which were compared using Student's *t*-test. Non-normally distributed variables are presented as medians (interquartile range). They were compared using the Mann–Whitney *U* test. Baseline categorical variables were compared using the Fisher's exact test or the χ^2 test, as appropriate. Intraclass correlation coefficients with 95% CIs were calculated to assess intraobserver and interobserver agreement for lipid arc, and kappa statistics were used to assess for agreement of plaque characterization.

Since several lipid-rich plaque-derived indices in the univariable analysis were highly correlated, we used variance inflation factor (VIF) analysis to measure the impact of collinearity among significant variables in the multivariable linear regression model as a continuous variable reflecting the precision of the estimate. Variables with VIF > 10 were omitted from the multivariable analyses due to high collinearity. Next, multivariable stepwise logistic regression analysis was performed using covariates that significantly predicted HIP with PMR > 1.4 in linear regression models plus established OCT indices for plaque vulnerability such as presence of TCFA, plaque rupture, macrophage accumulation, microchannel, and intracoronary thrombus and fibrous cap thickness. Stepwise selection with a *P*-value of 0.1 for backward elimination was used. All statistical tests were two-sided and *P*-values <0.05 were considered statistically significant. Statistical analysis was performed with JMP, version 11 (SAS Institute, Cary, NC, USA) and Stata, version 13 (StataCorp LP, College Station, TX, USA).

Results

Clinical characteristics, angiographic interpretation, OCT findings, and CTA measures

Of the 105 study patients, 44 (42%) patients had HIP lesions. Of these, two patients had more than one HIP lesion; these lesions were in non-culprit lesions in the same vessel as target lesions. Therefore, we analysed these lesions during OCT pullback. Ultimately, of 105 study patients, 44 patients (46 HIP lesions) were categorized into the HIP group and 61 patients (91 lesions) were categorized into the non-HIP group (Supplementary data online, *Table S1*).

For segment-based analysis, 703 of 840 segments (105 patients) on CMR images were excluded because they either contained non-target lesions in a coronary vessel that did not undergo PCI or were previously treated with PCI and stenting, leaving 137 segments in the analysis (*Figure 1*). Ultimately, plaques with PMR ≥1.4 were identified in 46 segments and plaques with PMR < 1.4 were observed in 91 segments.

Table 1 displays the clinical profiles of patients with and without HIP. There were no significant differences in age; gender; prevalence of hypertension, dyslipidaemia, diabetes mellitus; lipid profile; glycosylated haemoglobin levels; target vessel distribution; and medication use between the two groups. In particular, the proportion of patients taking statins was high and similar between the two groups.

Characteristics of OCT-verified plaques in the HIP and non-HIP lesions are presented in *Table 2*. There were no significant differences in the prevalence of TCFA, plaque rupture, calcification, microchannels, and intracoronary thrombus between the two groups. The prevalence of intracoronary thrombus was also similar in the two groups (11% in the HIP group and 8% in the non-HIP group, $P = 0.537$). Both groups demonstrated similar minimal fibrous cap thickness [180 μm (150–210) vs. 190 μm (150–220), $P = 0.180$]. On the other hand, HIP lesions had a higher frequency of lipid-rich plaque (96% vs. 70%, $P < 0.001$), macrophage accumulation (65% vs. 46%,

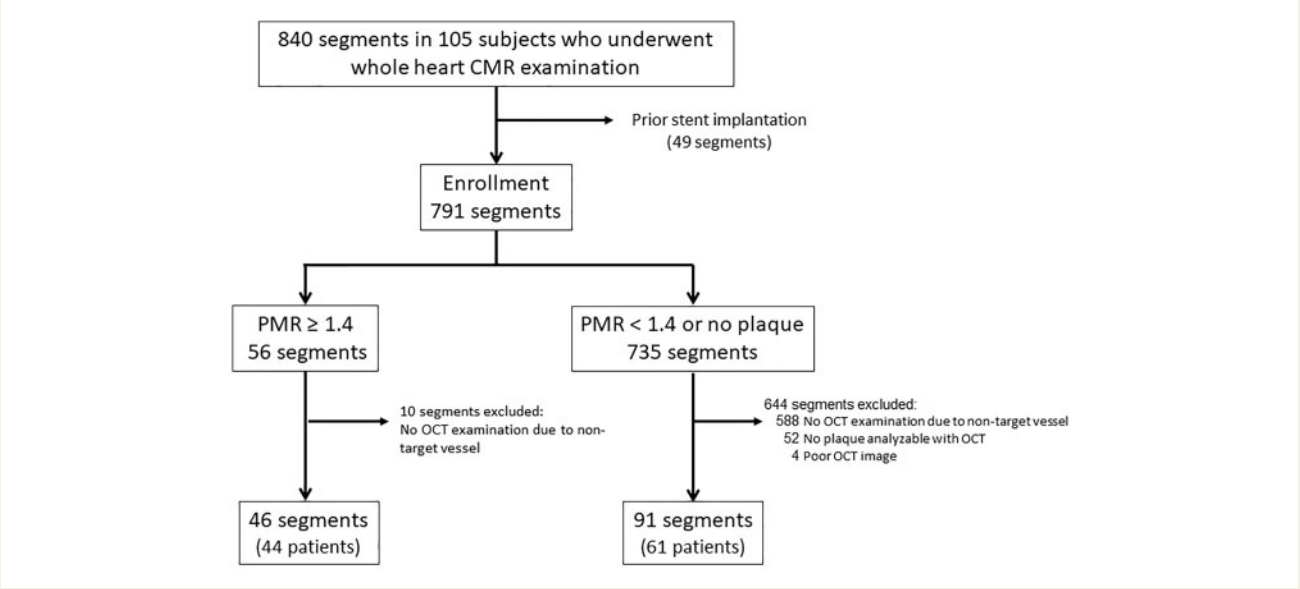

Figure 1 Segment-based analysis of CMR and OCT. A total of 791 segments were analysed. They were divided into 56 segments with a plaque-to-myocardial signal intensity ratio (PMR) ≥1.4 and 735 segments that have plaques with PMR <1.4. Of the 56 segments that have plaques with PMR ≥1.4, 10 segments were excluded due to being in non-culprit vessels that underwent PCI. Ultimately, 46 segments that have plaques with PMR ≥1.4 and 91 segments that have plaques with PMR <1.4 were included in the final analysis.

Table 1 Clinical characteristics and angiographic findings

	All patients ($n = 105$)	HIP ($n = 44$)	Non-HIP ($n = 61$)	*P*-value
Age (years)	67 ± 11	68 ± 10	65 ± 11	0.176
Male	88 (84)	37 (84)	51 (84)	1.000
Hypertension	78 (74)	37 (84)	41 (67)	0.070
Dyslipidaemia	91 (87)	39 (89)	52 (85)	0.773
Diabetes mellitus	40 (38)	16 (36)	24 (39)	0.840
Current smoker	15 (14)	5 (11)	10 (16)	0.577
BMI (kg/m^2)	24.4 ± 3.2	24.7 ± 3.4	24.2 ± 3.0	0.475
TC (mg/dL)	163 ± 34	163 ± 32	163 ± 36	0.899
LDL (mg/dL)	91 ± 31	89 ± 27	92 ± 33	0.961
HDL (mg/dL)	48 ± 12	48 ± 13	47 ± 12	0.773
TG (mg/dL)	138 ± 62	139 ± 60	137 ± 64	0.798
HbA1c (%)	6.2 ± 0.8	6.1 ± 0.8	6.2 ± 0.8	0.598
PMR	NA	1.77 (1.50, 2.20)	0.91 (0.83, 0.98)	<0.001
Medications				
Aspirin	103 (98)	43 (98)	60 (98)	1.000
Beta-blocker	61 (58)	28 (64)	33 (54)	0.423
ACEI/ARB	63 (60)	28 (64)	35 (57)	0.551
CCB	41 (39)	20 (45)	21 (34)	0.312
Statins	101 (96)	43 (98)	58 (95)	0.638
Target vessel ($n = 137$ segments)				0.885
LAD	84 (61)	27 (59)	57 (63)	
LCX	12 (9)	4 (9)	8 (9)	
RCA	41 (30)	15 (32)	26 (28)	

BMI, body mass index; ACEI, angiotensin converting enzyme inhibitor; ARB, angiotensin II receptor blocker; CCB, calcium channel blocker; HbA1c, glycosylated haemoglobin; HDL, high-density lipoprotein; HIP, high-intensity plaque; LAD, left anterior descending artery; LCX, left circumflex artery; LDL, low-density lipoprotein; NA, not applicable; PMR, plaque-to-myocardial signal intensity ratio; RCA, right coronary artery; TC, total cholesterol; TG, triglycerides.

Table 2 Optical coherence tomography analysis

	HIP (46 segments)	Non-HIP (91 segments)	*P*-value
Lipid-rich plaque	44 (96%)	64 (70%)	<0.001
Lipid length, mm	5.9 (4.7, 7.8)	3.6 (2.6, 4.6)	<0.001
Maximum lipid arc (°)	188 (169, 209)	139 (90, 173)	<0.001
Average lipid arc (°)	159 (133, 174)	99 (80, 147)	<0.001
Lipid index	895 (716, 1212)	336 (220, 635)	<0.001
Minimum fibrous cap thickness (μm)	180 (150, 210)	190 (150, 220)	0.180
TCFA	4 (9%)	4 (4%)	0.442
Healed plaque rupture	33 (72%)	16 (18%)	<0.001
Plaque rupture	6 (13%)	14 (15%)	0.802
Calcification	14 (30%)	36 (40%)	0.350
Thrombus	5 (11%)	7 (8%)	0.537
Red thrombus	1 (20%)	1 (14%)	
White thrombus	4 (80%)	6 (86%)	
Macrophage accumulation	30 (65%)	42 (46%)	0.046
Cholesterol crystal	21 (46%)	20 (22%)	0.006
Microchannel	20 (43%)	31 (34%)	0.349

HIP, high-intensity plaque; TCFA, thin cap fibroatheroma.

$P = 0.046$), cholesterol crystals (46% vs. 22%, $P = 0.006$), and healed plaque rupture (72% vs. 18%, $P < 0.001$) compared with non-HIP lesions. Compared with non-HIP lesions, the HIP lesions had a wider lipid arc [188° (169–209) vs. 139° (90–173), $P < 0.001$] and a longer lipid length [5.9 mm (4.7–7.8) vs. 3.6 mm (2.6–4.6), $P < 0.001$]. Representative cases of HIP and non-HIP lesions and corresponding OCT images are shown in *Figures 2 and 3*.

PMR was positively correlated with maximum lipid arc ($r = 0.457$, $P < 0.001$) (*Figure 4A*), lipid length ($r = 0.540$, $P < 0.001$) (*Figure 4B*), and lipid index ($r = 0.588$, $P < 0.001$) (*Figure 4C*), but not fibrous cap thickness (*Figure 4D*). As reported previously,[2] we divided target lesions into high (PMR ≥ 1.4), medium (PMR 1.0–1.4), and low (PMR < 1.0) PMR groups. In the high PMR group 72% of lesions had healed plaque rupture compared with 27% in the medium group and 13% in the low PMR group (*Figure 5*).

The comparison of CTA measures between HIPs and non-HIPs is summarized in Supplementary data online, *Table S4*. The median RI in the HIP group was significantly higher than in the non-HIP group [1.24 (1.08–1.40) vs. 0.99 (0.91–1.12), $P < 0.001$]. Positive remodelling was observed in 42 (91.3%) of 46 segments with HIPs, as opposed to 13 (14.3%) of 91 segments with non-HIPs. In addition, total atheroma volume and LAP volume were significantly larger in HIPs [199.8 (148.5–265.2) mm^3 vs. 100.8 (68.2–130.3) mm^3, $P < 0.001$; 27.3 (15.4–49.6) mm^3 vs. 6.7 (3.4–12.1) mm^3, $P < 0.001$, respectively]. The frequency of spotty calcification was not statistically significant (41.3% vs. 30.8%, $P = 0.061$).

Factors related to the presence of HIP

Univariable analysis of OCT characteristics showed that lipid-rich plaque, lipid length, maximum lipid arc, average lipid arc, healed plaque rupture, and cholesterol crystal were all significant predictors of HIP ($P < 0.01$). These variables were further analysed in a multivariable linear regression model with VIF analysis. Lipid length, maximum lipid arc, and average lipid arc were omitted from the VIF analysis because of collinearity. After stepwise selection to adjust for factors that were significant in the univariable analysis and known OCT-derived high-risk morphological features (TCFA, plaque rupture, calcification, thrombus, macrophage accumulation, microchannel), presence of healed plaque rupture remained a significant independent predictor of HIP (*Table 3*, Model 1). To remove insignificant variables from Model 1 for parsimony, multivariable stepwise selection analysis was performed. As a result, both the presence of lipid-rich plaque [odds ratio (OR) 4.38; 95% CI 1.08–29.77; $P = 0.038$] and healed plaque rupture (OR 9.32; 95% CI 4.05–22.71; $P < 0.001$) were identified as significant determinants of HIP (*Table 3*, Model 2). In contrast, the presence of intracoronary thrombus, TCFA, and fibrous cap thickness were not associated with HIP. Thus, multivariable stepwise logistic regression analysis showed that the presence of HIP was most significantly associated with lipid-rich plaque and healed plaque rupture.

Interobserver and intraobserver variability for plaque characterization

The interval between initial analysis of OCT-derived features and secondary analysis was 1 month. Intraclass correlation coefficients with 95% CIs for interobserver and intraobserver reliability for lipid arc were 0.87 (95% CI 0.73–0.93) and 0.91 (0.79–0.95), respectively. There was acceptable interobserver concordance for intracoronary thrombus ($\kappa = 0.89$), healed plaque rupture ($\kappa = 0.73$), lipid-rich plaque ($\kappa = 0.69$), and TCFA ($\kappa = 0.73$). There also was acceptable intraobserver concordance for intracoronary thrombus ($\kappa = 0.92$), healed plaque rupture ($\kappa = 0.73$), lipid-rich plaque ($\kappa = 0.82$), and TCFA ($\kappa = 0.87$).

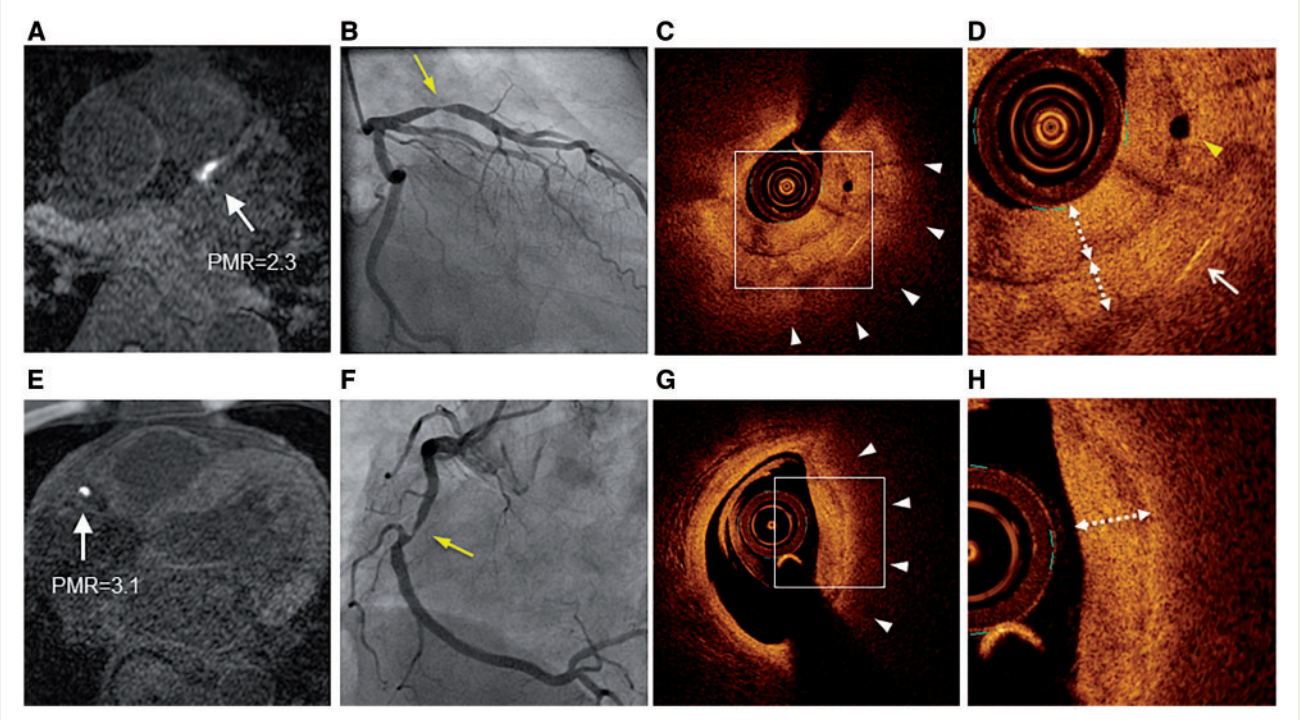

Figure 2 Representative HIP lesions on T1-weighted imaging and optical coherence tomography. Non-contrast T1-weighted imaging (T1WI) demonstrated HIPs (white arrows) in the proximal left anterior descending artery (*A*) and in the middle of the right coronary artery (*E*). These lesions had PMR of 2.3 and 3.1, respectively. Coronary artery angiography revealed significant coronary stenosis in lesions corresponding to HIPs (*B* and *F*) (yellow arrows). Optical coherence tomography (OCT) showed a layered signal pattern underlying a signal-poor region with diffuse borders (white arrowheads) in the areas corresponding to each HIP (*C* and *G*). The white dotted line with double arrows indicates the layered pattern of OCT signals in high-power images (*D* and *H*). The yellow arrowhead indicates a microchannel (D). The white arrow indicates a cholesterol crystal (D). HIPs, high-intensity plaques; PMR, plaque-to-myocardium signal intensity ratio.

Discussion

HIP and healed plaque rupture

In the present study of patients with stable CAD, OCT-verified presence of healed plaque rupture and lipid-rich plaque were associated with HIP regardless of intracoronary thrombus status. Healed plaque rupture is pathologically characterized as a disrupted fibrous cap consisting of collagen type I with an underlying necrotic core and an overlying repair reaction, typically consisting of smooth muscle cells, proteoglycan, and collagen type III.[8] Healed plaque rupture can be detected by OCT as a layered pattern of signals with an underlying signal-poor region[9] (*Figure 2*). Since episodic rupture and healing potentially contribute to increased lipid burden and luminal narrowing, it is conceivable that the presence of healed plaque rupture itself may reflect an increased risk of future events. A previous autopsy study had reported that in patients with sudden coronary death, the prevalence of healed plaque rupture was 80% in hearts with stable plaque and healed myocardial infarction.[7] Higher numbers of healed plaque rupture sites might be associated with larger necrotic cores and higher plaque volume. During healing of disrupted plaques, thrombus is incorporated into the repaired territory. Dying red blood cells produce substantial amounts of free cholesterol and cholesterol crystals, which contribute to higher lipid content in the plaque.[22] However, further clinical studies are warranted to investigate whether healed plaque rupture contributes to plaque progression.

In addition to healed plaque rupture, HIP was also significantly associated with the presence of lipid-rich plaque, and PMR was positively correlated with maximum lipid arc and lipid length (*Figure 4A–C*). These findings were consistent with a previous intravascular ultrasound study of patients with stable CAD that showed a significantly higher prevalence of a lipid pool in patients with HIP. The presence of a lipid pool was strongly correlated with periprocedural myocardial infarction.[3]

Importantly, no significant differences were observed in the presence of TCFA, microchannels, and plaque rupture between the HIP and non-HIP groups in this study (*Table 2*). Our present findings are markedly different from those in previous OCT studies that involved mostly ACS patients.[14,23] Kubo *et al.*[24] reported that in infarct-related or PCI target lesions in patients with acute myocardial infarction (AMI) or SAP, OCT-derived plaque rupture (AMI 77% vs. SAP 7%, $P < 0.001$) and intracoronary thrombus (AMI 100% vs. SAP 0%, $P < 0.001$) were observed more frequently in AMI than in SAP. In addition, the frequency of OCT-derived TCFA was significantly lower in SAP than in AMI (SAP 6% vs. AMI 38%, $P = 0.03$). Consistent with these previous imaging studies, the composition of HIP is different in patients with stable CAD or silent myocardial infarction vs. patients with ACS.

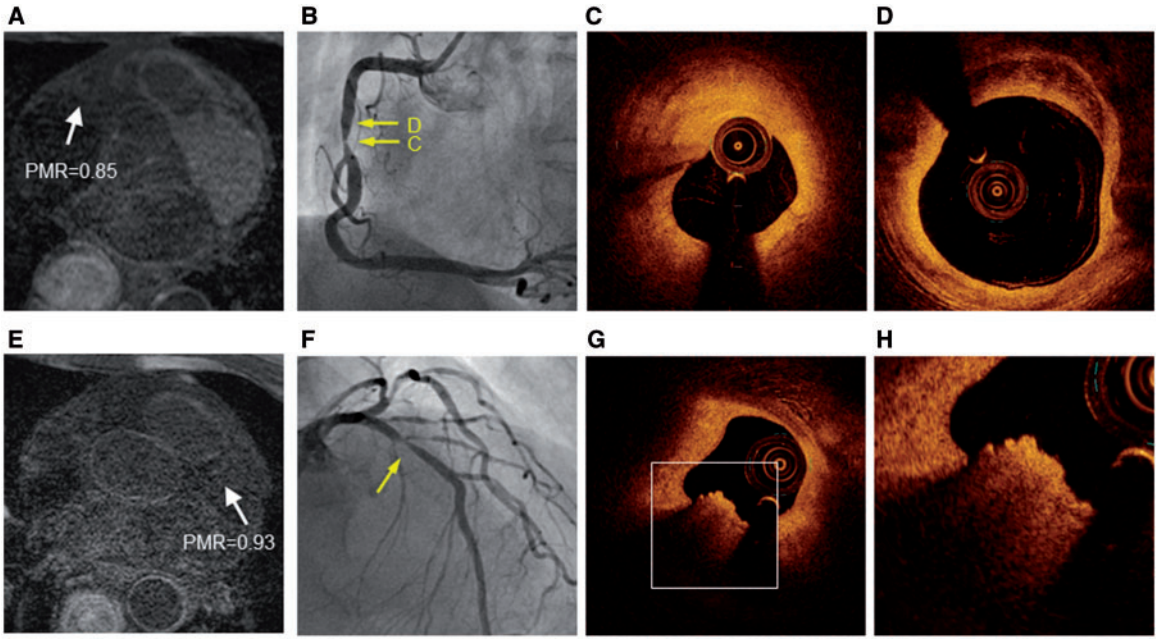

Figure 3 Representative non-HIP lesions on T1-weighted imaging with corresponding optical coherence tomography. Representative non-HIPs (white arrows) in the middle of the right coronary artery (PMR, 0.85) (*A*) and proximal left anterior descending artery (PMR, 0.93) (*E*). Coronary artery angiography revealed significant coronary stenosis (*B* and *F*) (yellow arrows). Optical coherence tomography showed that the target lesion was predominately comprised of fibrous plaque without attenuation (*C* and *D*). A typical red thrombus was observed in a non-HIP area (*G*). A higher power image of the white square in (G) is shown in (*H*). HIPs, high-intensity plaques; PMR, plaque-to-myocardium signal intensity ratio.

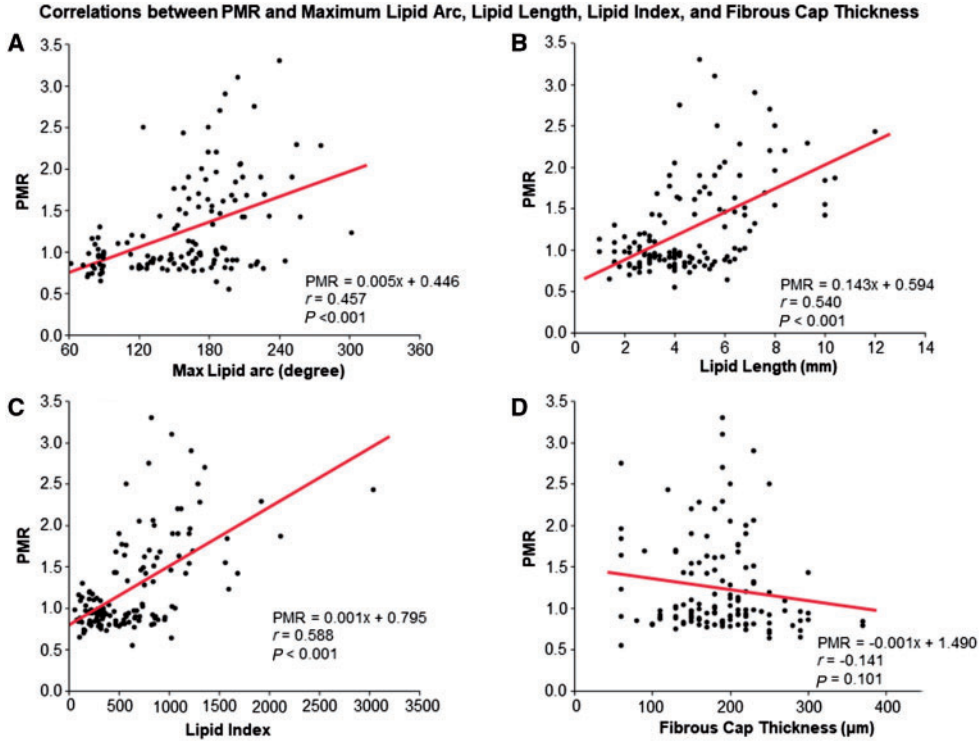

Figure 4 Correlations between PMR and maximum lipid arc, lipid length, and fibrous cap thickness. PMR was positively correlated with maximum lipid arc (*A*), lipid length (*B*) and lipid index (*C*), but not fibrous cap thickness (*D*). HIPs, high-intensity plaques; PMR, plaque-to-myocardium signal intensity ratio.

Potential mechanisms for high signal intensity in coronary plaques

In previous carotid MR studies, the presence of lesions with high-intensity signal was considered to indicate intraplaque haemorrhage (IPH) that contributes to a significant shortening of T1 relaxation time. Because IPH often occurs within necrotic cores, lipid-rich core regions also contribute to high-intensity signals on T1WI.[25,26] The histopathological basis of these associations has been demonstrated in carotid endarterectomy specimens.[25,27] In coronary lesions, we have demonstrated that HIPs with high PMR are associated with adverse outcomes.[2] Since the presence of HIP in a coronary artery is considered to indicate a necrotic core with IPH, the association between coronary HIP and increased risk of future cardiovascular events may be partly attributable to IPH involvement. Aspiration of coronary specimens corresponding to coronary HIP visualized on a 3 T MR system has confirmed that a large portion of the necrotic core has fibrin-rich thrombus and numerous immunohistologically confirmed CD68+ macrophages.[12] Intraluminal thrombus has also been previously shown to be associated with coronary HIP in patients with ACS based on intravascular OCT or specimens obtained through an aspiration catheter during PCI.[14,18,23] Along with the present OCT findings in patients with stable CAD, HIP seems to represent several important components of pathologically advanced plaques. However, the actual cause of high signal intensity in atherosclerotic coronary plaques on T1WI remains under discussion. Further studies are needed to clarify the coronary plaque characteristics representing HIP on non-contrast T1WI.

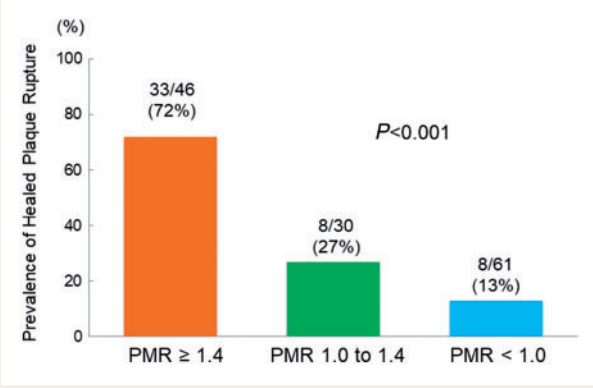

Figure 5 Prevalence of healed plaque rupture categorized by PMR. The prevalence of healed plaque rupture was significantly higher in the PMR > 1.4 group than in other groups.

Study limitations

The number of subjects in this study was small. In addition, recruiting patients with significant coronary stenosis might have resulted in selection bias. Since OCT has limited axial penetration depth (≤2.0 mm), we could not evaluate the number of layers overlying a large necrotic core when evaluating healed plaque rupture, vascular remodelling index, and total lipid volume. However, CTA helped overcome some limitations of OCT in HIP characterization. Namely, the HIP group had a significantly higher prevalence of positive remodelling, larger total atheroma volume, and larger LAP volume (Supplementary data online, *Table S4*).

OCT findings in HIP and non-HIP lesions overlap, although OCT allows us to visualize the micromorphology of coronary arteries with near-histological resolution. Since OCT findings and histopathological data were not directly compared in this study, the precise characteristics of HIPs remain unknown. The development of atherosclerosis is a continuous process that involves numerous interconnected cellular and acellular processes that influence the behaviour of each other.

Table 3 Association between HIP and OCT-derived parameters based on univariable and multivariable logistic regression analysis

	Univariable analysis			Multivariable analysis: Model 1			Multivariable analysis: Model 2		
	OR	95% CI	*P*-value	OR	95% CI	*P*-value	OR	95% CI	*P*-value
Lipid-rich plaque	9.28	2.60–59.37	<0.001	3.34	0.73–24.16	0.125	4.38	1.08–29.77	0.038
Lipid length (mm)	2.24	1.72–3.08	<0.001						
Maximum lipid arc (°)	1.03	1.02–1.04	<0.001						
Average lipid arc (°)	1.03	1.02–1.05	<0.001						
Lipid index	1.42	1.21–1.80	<0.001						
Minimum fibrous cap thickness (μm)	1.00	0.99–1.00	0.091	1.00	0.99–1.01	0.486			
TCFA	2.07	0.47–9.15	0.324	5.69	0.71–47.33	0.101			
Healed plaque rupture	11.74	5.21–28.11	<0.001	11.30	4.55–33.15	<0.001	9.32	4.05 –22.71	<0.001
Plaque rupture	0.83	0.28–2.23	0.712	0.75	0.21–2.63	0.652			
Calcification	0.67	0.31–1.41	0.291	1.13	0.41–3.05	0.808			
Thrombus	0.88	0.23–3.34	0.855	1.96	0.40–9.69	0.404			
Macrophage accumulation	2.18	1.06–4.63	0.034	1.62	0.64–4.21	0.309			
Cholesterol crystal	2.98	1.40–6.46	0.005	1.67	0.63–4.43	0.304			
Microchannel	1.48	0.72–3.08	0.283	1.29	0.52–3.21	0.576			

CI, confidence interval; HIP, high-intensity plaque; OCT, optical coherence tomography; OR, odds ratio; TCFA, thin cap fibroatheroma.

The precise roles of many of these processes are unknown, and further studies are needed.

Given the observational nature of our present study, there might have been selection bias due to patient recruitment in a single centre. In addition, we did not explore the entire coronary tree using OCT imaging. Therefore, the exclusion of some non-target lesions might have introduced some bias.

Conclusions

HIP on non-contrast T1WI in patients with stable CAD is strongly associated with healed plaque rupture and a large lipid core as detected by OCT. These findings suggest the morphological basis of HIP and explain the high-risk nature of HIP with high PMR.

Supplementary data

Supplementary data are available at *European Heart Journal - Cardiovascular Imaging* online.

Funding

The present work was supported in part by grants from the Takeda Science Foundation and the Japan Cardiovascular Research Foundation.

Conflict of interest: None declared.

References

1. Noguchi T, Yamada N, Kawasaki T, Tanaka A, Yasuda S. Detection of high-risk atherosclerotic plaques by magnetic resonance imaging. *Circ J* 2013;**77**:1975–83.
2. Noguchi T, Kawasaki T, Tanaka A, Yasuda S, Goto Y, Ishihara M *et al.* High-intensity signals in coronary plaques on noncontrast T1-weighted magnetic resonance imaging as a novel determinant of coronary events. *J Am Coll Cardiol* 2014;**63**:989–99.
3. Hoshi T, Sato A, Akiyama D, Hiraya D, Sakai S, Shindo M *et al.* Coronary high-intensity plaque on T1-weighted magnetic resonance imaging and its association with myocardial injury after percutaneous coronary intervention. *Eur Heart J* 2015;**36**:1913–22.
4. Kume T, Akasaka T, Kawamoto T, Ogasawara Y, Watanabe N, Toyota E *et al.* Assessment of coronary arterial thrombus by optical coherence tomography. *Am J Cardiol* 2006;**97**:1713–7.
5. Tearney GJ, Yabushita H, Houser SL, Aretz HT, Jang IK, Schlendorf KH *et al.* Quantification of macrophage content in atherosclerotic plaques by optical coherence tomography. *Circulation* 2003;**107**:113–9.
6. Yabushita H, Bouma BE, Houser SL, Aretz HT, Jang IK, Schlendorf KH *et al.* Characterization of human atherosclerosis by optical coherence tomography. *Circulation* 2002;**106**:1640–5.
7. Burke AP, Kolodgie FD, Farb A, Weber DK, Malcom GT, Smialek J *et al.* Healed plaque ruptures and sudden coronary death: evidence that subclinical rupture has a role in plaque progression. *Circulation* 2001;**103**:934–40.
8. Mann J, Davies MJ. Mechanisms of progression in native coronary artery disease: role of healed plaque disruption. *Heart* 1999;**82**:265–8.
9. Otsuka F, Joner M, Prati F, Virmani R, Narula J. Clinical classification of plaque morphology in coronary disease. *Nat Rev Cardiol* 2014;**11**:379–89.
10. Yahagi K, Kolodgie FD, Otsuka F, Finn AV, Davis HR, Joner M *et al.* Pathophysiology of native coronary, vein graft, and in-stent atherosclerosis. *Nat Rev Cardiol* 2016;**13**:79–98.
11. Asaumi Y, Noguchi T, Morita Y, Fujiwara R, Kanaya T, Matsuyama TA *et al.* High-intensity plaques on noncontrast T1-weighted imaging as a predictor of periprocedural myocardial injury. *JACC Cardiovasc Imaging* 2015;**8**:741–3.
12. Asaumi Y, Noguchi T, Morita Y, Matsuyama TA, Otsuka F, Fujiwara R *et al.* Noncontrast T1-weighted magnetic resonance imaging at 3.0 Tesla in a patient undergoing elective percutaneous coronary intervention—clinical and pathological significance of high-intensity plaque. *Circ J* 2014;**79**:218–20.
13. Kawasaki T, Koga S, Koga N, Noguchi T, Tanaka H, Koga H *et al.* Characterization of hyperintense plaque with noncontrast T(1)-weighted cardiac magnetic resonance coronary plaque imaging: comparison with multislice computed tomography and intravascular ultrasound. *JACC Cardiovasc Imaging* 2009;**2**:720–8.
14. Matsumoto K, Ehara S, Hasegawa T, Sakaguchi M, Otsuka K, Yoshikawa J *et al.* Localization of coronary high-intensity signals on T1-weighted MR imaging: relation to plaque morphology and clinical severity of angina pectoris. *JACC Cardiovasc Imaging* 2015;**8**:1143–52.
15. Kataoka Y, Puri R, Hammadah M, Duggal B, Uno K, Kapadia SR *et al.* Sex differences in nonculprit coronary plaque microstructures on frequency-domain optical coherence tomography in acute coronary syndromes and stable coronary artery disease. *Circ Cardiovasc Imaging* 2016;**9**:pii: e004506.
16. Kume T, Akasaka T, Kawamoto T, Watanabe N, Toyota E, Neishi Y *et al.* Assessment of coronary arterial plaque by optical coherence tomography. *Am J Cardiol* 2006;**97**:1172–5.
17. Tearney GJ, Regar E, Akasaka T, Adriaenssens T, Barlis P, Bezerra HG *et al.* Consensus standards for acquisition, measurement, and reporting of intravascular optical coherence tomography studies: a report from the International Working Group for Intravascular Optical Coherence Tomography Standardization and Validation. *J Am Coll Cardiol* 2012;**59**:1058–72.
18. Ehara S, Hasegawa T, Nakata S, Matsumoto K, Nishimura S, Iguchi T *et al.* Hyperintense plaque identified by magnetic resonance imaging relates to intracoronary thrombus as detected by optical coherence tomography in patients with angina pectoris. *Eur Heart J Cardiovasc Imaging* 2012;**13**:394–9.
19. Motoyama S, Sarai M, Harigaya H, Anno H, Inoue K, Hara T *et al.* Computed tomographic angiography characteristics of atherosclerotic plaques subsequently resulting in acute coronary syndrome. *J Am Coll Cardiol* 2009;**54**:49–57.
20. Noguchi T, Tanaka A, Kawasaki T, Goto Y, Morita Y, Asaumi Y *et al.* Effect of intensive statin therapy on coronary high-intensity plaques detected by noncontrast T1-weighted imaging: the AQUAMARINE pilot study. *J Am Coll Cardiol* 2015;**66**:245–56.
21. Watabe H, Sato A, Akiyama D, Kakefuda Y, Adachi T, Ojima E *et al.* Impact of coronary plaque composition on cardiac troponin elevation after percutaneous coronary intervention in stable angina pectoris. A computed tomography analysis. *J Am Coll Cardiol* 2012;**59**:1881–8.
22. Kolodgie FD, Gold HK, Burke AP, Fowler DR, Kruth HS, Weber DK *et al.* Intraplaque hemorrhage and progression of coronary atheroma. *N Engl J Med* 2003;**349**:2316–25.
23. Jansen CH, Perera D, Makowski MR, Wiethoff AJ, Phinikaridou A, Razavi RM *et al.* Detection of intracoronary thrombus by magnetic resonance imaging in patients with acute myocardial infarction. *Circulation* 2011;**124**:416–24.
24. Kubo T, Imanishi T, Kashiwagi M, Ikejima H, Tsujioka H, Kuroi A *et al.* Multiple coronary lesion instability in patients with acute myocardial infarction as determined by optical coherence tomography. *Am J Cardiol* 2010;**105**:318–22.
25. Moody AR, Murphy RE, Morgan PS, Martel AL, Delay GS, Allder S *et al.* Characterization of complicated carotid plaque with magnetic resonance direct thrombus imaging in patients with cerebral ischemia. *Circulation* 2003;**107**:3047–52.
26. Yuan C, Mitsumori LM, Ferguson MS, Polissar NL, Echelard D, Ortiz G *et al.* In vivo accuracy of multispectral magnetic resonance imaging for identifying lipid-rich necrotic cores and intraplaque hemorrhage in advanced human carotid plaques. *Circulation* 2001;**104**:2051–6.
27. Stary HC, Chandler AB, Dinsmore RE, Fuster V, Glagov S, Insull W, Jr *et al.* A definition of advanced types of atherosclerotic lesions and a histological classification of atherosclerosis. A report from the Committee on Vascular Lesions of the Council on Arteriosclerosis, American Heart Association. *Circulation* 1995;**92**:1355–74.